ORGANOMETALLICS Article

Cite This: *Organometallics* XXXX, XXX, XXX−XXX

Monitoring of the Phosphine Role in the Mechanism of Palladium-Catalyzed Benzosilole Formation from Aryloxyethynyl Silanes

Martí Gimferrer,[†] Yasunori Minami,*[,‡] Yuta Noguchi,[§] Tamejiro Hiyama,[‡] and Albert Poater*[,†]

[†]Institut de Química Computacional i Catàlisi and Departament de Química, Universitat de Girona, Campus Montilivi, 17003 Girona, Catalonia, Spain

[‡]Research and Development Initiative, Chuo University, 1-13-27, Kasuga, Bunkyo-ku, Tokyo 112-8551, Japan

[§]Department of Applied Chemistry, Chuo University, 1-13-27, Kasuga, Bunkyo-ku, Tokyo 112-8551, Japan

Supporting Information

ABSTRACT: Understanding the formation of benzosiloles by the intramolecular palladium-catalyzed annulation of alkynyl(aryl)silanes is crucial for achieving synthetic diversity toward the enhancement of the chemistry of siloles. By a combination of density functional theory calculations and experiments, we describe not only the whole mechanism of reaction but also the drawbacks that block this type of reaction. We also unravel the role of the phosphine ligand, without which the reactions could not go forward. Moreover, in silico predictive catalysis is presented here since the substitution of the phosphine ligand by an N-heterocyclic carbene (NHC) promises milder experimental conditions. A screening of substrates with different electronic properties was carried out to further understand the two fundamental steps of the reaction: stereoisomerization and concerted metalation−deprotonation.

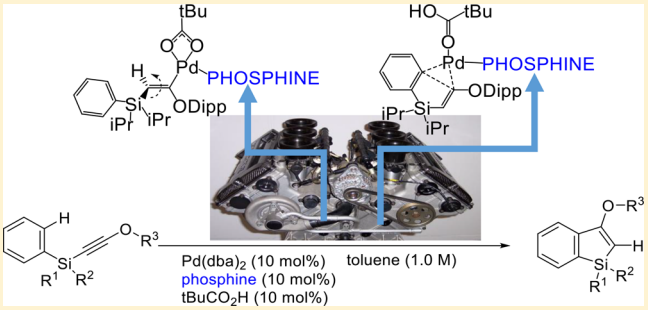

INTRODUCTION

Substituting carbon by silicon atoms on an organic compound drastically modifies its chemical and physicochemical properties, opening, for the resulting silicon-based compounds, the gate to potential applications including high-electron-affinity materials, building blocks for organic synthesis, and solid-state luminescence. For this reason, in recent years interest in organic π-conjugated molecules with silicon atoms incorporated[1,2] has increased. Consequently, numerous catalytic reactions for their preparation[3,4] have been reported, including the formation of dibenzo-[5,6] and benzosiloles.[7] In comparison with the dibenzosilole formation, there are only a few synthetic strategies developed that give access to benzosiloles, on the basis of metal-catalyzed annulation protocols: (a) cyclization of *o*-alkynylphenylsilanes via anulation with additives such as electrophiles,[8] (b) annulation of aryl vinyl silanes via Mizoroki−Heck reactions[9] or Grubbs olefin metathesis catalysts,[10] (c) intramolecular C−H ortho silylation,[11] (d) annulation of alkynes with arylsilanes via Si−H bond cleavage,[12] and (e) trans-hydroarylation by alkynyl aryl silanes.[13]

Among the benzosilole formation reactions, the majority require the transformation of the Si−C bond, which often acts as a key step.[14,15] Computationally, Si−C bond cleavage was studied using rhodium-based transition-metal complexes.[16] Alternatively, in 2016, Minami et al. achieved the synthesis of benzosiloles by palladium-/acid-catalyzed intramolecular anti-hydroarylation of alkynyl(aryl)silanes (see Scheme 1).[13] Due to the simplicity of synthesizing the silane reagents, an understanding of the reaction mechanism is crucial to achieve synthetic diversity toward the enhancement of the chemistry of siloles. For this purpose, in the current work we present a computational study by density functional theory (DFT) calculations of the full reaction mechanism for benzosilole formation from aryloxyethynyl silane reagents, investigating also the role of the phosphine ligand and disclosing the drawbacks which block this type of reaction.

Scheme 1. Palladium-Catalyzed Anti-Hydroarylation Using Alkynyl(aryl)Silanes for Benzosilole Formation[13]

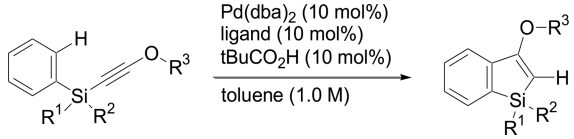

RESULTS AND DISCUSSION

The full reaction mechanism of the formation of the benzosilole **P** from the aryloxyethynyl silane **R** is depicted in Figure 1. For the sake of simplicity, the experimentally used triethylphosphine (PEt_3) was replaced by trimethylphosphine (PMe_3). Once both dba ligands of the $Pd(dba)_2$ catalyst were substituted by a PMe_3 ligand and a pivalic acid, with a minimal

Received: February 20, 2018

DOI: 10.1021/acs.organomet.8b00102
Organometallics XXXX, XXX, XXX−XXX

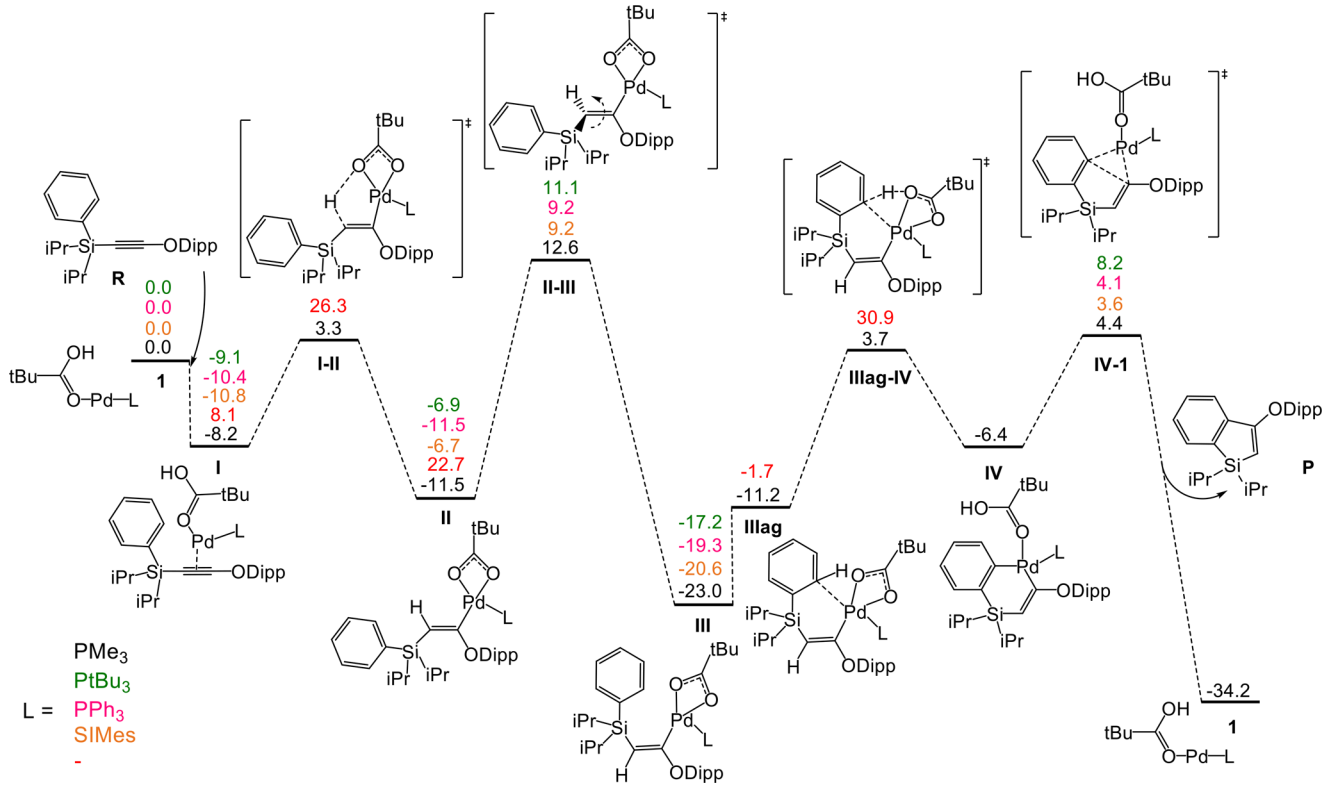

Figure 1. Full reaction pathway for Pd-catalyzed benzosilole formation from aryloxyethynyl silane, including selected values for ligands alternative to PMe_3 (M06/cc-pVTZ~sdd//BP86-d3/SVP~sdd; Gibbs free energies referenced to complex **1** in kcal/mol).

loss of energy of 0.2 kcal/mol, whereas the species in between, Pd(dba)(PMe_3), is only 0.8 kcal/mol higher in energy, the first step consists of the π coordination of the aryloxyethynyl silane **R** to the pivalic Pd(0) complex **1** to form **I**.[17] Then, a syn-hydropalladation[18] occurs, providing the vinyl palladium pivalate **II**. The formation energy of **II** is strongly dependent on the presence of the phosphine ligand. For instance, **II** is almost 12 kcal/mol lower and 23 kcal/mol higher in energy than **1**+**R** when the phosphine is coordinated to Pd or when the phosphine is absent, respectively. Once the *E* complex **II** is achieved, the formation of the *Z* complex **III** takes place via stereoisomerization,[19,20] overcoming an energy barrier of 24.1 kcal/mol. This transition state **II-III** is based on the rotation of the C−C bond (dihedral angle of 84°; see Figure 2a).

The next step consists of a concerted metalation−deprotonation (CMD), which can be separated into the barrierless formation of an agostic interaction between the metallic center and an ortho carbon of the phenyl group (**IIIag**) and hydrogen transfer from the phenyl to the pivalate ligand (**IIIag-IV**). The latter transition state **IV-1** finishes the annulation process (see Figure 2b). Once the metallacycle **IV** is obtained, a reductive elimination occurs, restoring the catalytically active species **1** and forming the benzosilole product **P**. The energy required to overcome the barrier defined by the transition state **IV-1** is rather low (less than 11 kcal/mol); however, that calculated from the intermediate **III** turns out to be 27.4 kcal/mol bearing PMe_3 as a phosphine. Consequently, this is the rate-determining step (rds) of the whole reaction pathway.

In previous studies, it was assumed that the isomerization occurs (1) due to the steric repulsion of the Dipp and the two isopropyl groups on silicon and (2) by the donation of the lone pair electrons from the oxygen atom to the C−C double bond. We demonstrate here that the electronic properties and the sterics of the phosphine ligand (see Scheme 2) affect the energy barrier corresponding to this step, spanning from 15.9 kcal/mol for the SIMes ligand to 24.1 kcal/mol for the PMe_3 ligand. Then, the choice of the phosphine ligand is crucial to reduce the energy required to overcome the transition state **II-III** that leads to intermediate **III**, and this becomes rather facile with more sterically hindered ligands, such as $PtBu_3$ and SIMes.[21]

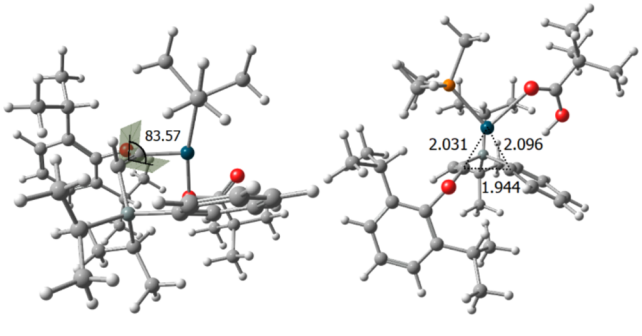

Figure 2. DFT-optimized geometries for the transition states (a) **II-III** and (b) **IV-1** with the main distances given in Å.

Scheme 2. Catalyst Screening for Benzosilole Formation

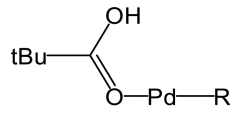

R = PMe_3 R = PPh_3
R = PEt_3 R = SIMes
R = $PtBu_3$ R = -

DOI: 10.1021/acs.organomet.8b00102
Organometallics XXXX, XXX, XXX−XXX

For the rds, defined by the transition state **IV-1**, the step requires roughly at least 25 kcal/mol independently of the phosphine ligand used, and this barrier hardly decreases using SIMes. Thus, even though the rds is not that affected by the nature of the phosphine, more sterically demanding phosphines facilitate this step, with energy barriers of 27.4 and 25.4 kcal/mol, for PMe_3 and $PtBu_3$, respectively. Overall, the catalytic cycle is strongly exergonic (34.2 kcal/mol).

An alternative pathway for the formation of intermediate **II**, again starting from the catalytic species **1**, was also tested (see Figure 3). First, an intramolecular oxidative addition occurs,

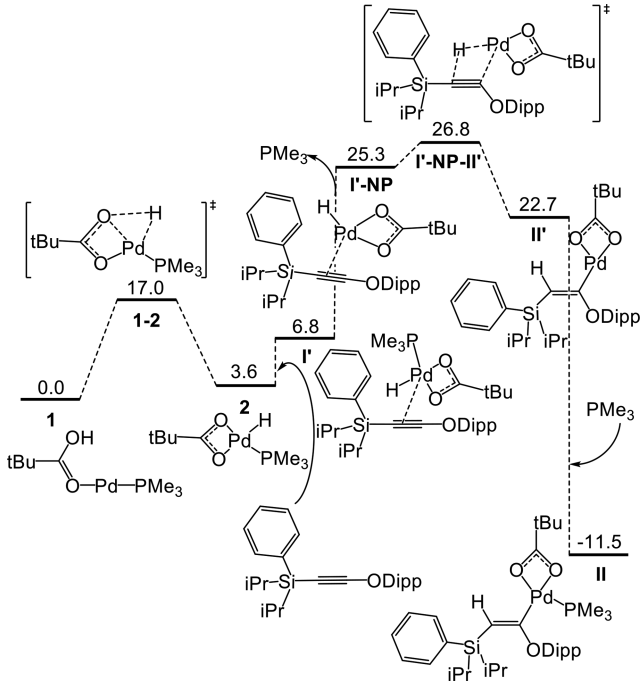

Figure 3. Alternative pathway for the formation of intermediate **II** (M06/cc-pVTZ~sdd//BP86-d3/SVP~sdd; Gibbs free energies in kcal/mol referenced to complex **1**).

transferring the hydrogen from the pivalic acid ligand to the metallic center, oxidizing the Pd(0) metal center to +2. This step forms the pivalate-coordinated square-planar complex **2** for an energy cost of 17.0 kcal/mol. It is important to mention that the thermodynamic equilibrium here is slightly displaced to the former species **1**, by 3.6 kcal/mol. Next, the aryloxyethynyl silane **R** approaches intermediate **2**, forming the relatively unstable intermediate **I′**, which is even 3.2 kcal/mol less stable than **2**. Then, the phosphine ligand dissociates (**I′-NP**), with a thermodynamic cost of 18.5 kcal/mol, which reduces the steric hindrance around the metal sphere, allowing the metallic center of the square planar moiety to achieve the desired π coordination with the alkyne reagent. Finally, species **I′-NP** undergoes a syn-hydropalladation that leads to intermediate **II′**, followed by the recoordination of the phosphine ligand leading to intermediate **II**, which species is shared for both reaction pathways. Overall, kinetically this alternative pathway requires 26.8 kcal/mol to form intermediate **II**, whereas in the general pathway in Figure 1 only 11.5 kcal/mol is required.

We expanded the mechanistic study to other aryloxyethynyl silane substrates (see Scheme 3), focusing on the energy barriers of the three fundamental steps of the mechanistic cycle: i.e., syn-hydropalladation, stereoisomerization, and C−C bond

Scheme 3. Substrate Screening for Benzosilole Formation

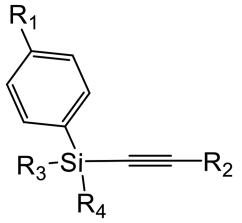

	R_1	R_2	R_3	R_4
a	H	ODipp	*i*Pr	*i*Pr
b	OMe	ODipp	*i*Pr	*i*Pr
c	NPh_2	ODipp	*i*Pr	*i*Pr
d	CF_3	ODipp	*i*Pr	*i*Pr
e	NO_2	ODipp	*i*Pr	*i*Pr
f	H	ODipp	*t*Bu	Ph
g	H	Ph	*t*Bu	Ph
h	H	OCH_2*t*Bu	*t*Bu	Ph
i	H	O-3-5-Xyl	*t*Bu	Ph
j	H	ODipp	H	H
k	H	ODipp	H	*i*Pr
l	H	ODipp	CH_3	CH_3

formation that leads to the cyclized organic product **P**. First, we substituted the para position of the phenyl group of the reagent **R** by electron-donating (ED) and -withdrawing (EW) substituents, having methoxy and diphenylamine of ED character and trifluoromethyl and nitro as EW moieties. Second, we substituted the isopropyl groups on Si by bulkier ones; finally, the ODipp substituent was substituted by carbon-coordinated species. Thus, we would see to what extent the sterics and the electronic character of the substituents affect the reactivity. The results obtained for the different substrates, referenced to the corresponding former species, are compiled in Table 1.

For the substrates with the phenyl group differently para substituted, we observed that the stereoisomerization and *syn*-hydropalladation steps of the reaction are unaffected by the electronic character of the substituents, presenting in all cases energy barriers of around 22.0−25.0 and 11.0−12.0 kcal/mol, respectively. The NPh_2 case will be discussed below. For the rate-determining step, the electron-donating groups OMe and NPh_2 impose higher energy barriers in comparison to the electron-withdrawing groups CF_3 and NO_2. However, the difference in the energy barriers is at least 2 kcal/mol, making it very difficult to determine if the difference is caused by the electronic character of the substituents or by the different repulsive/attractive interactions from each moiety with the rest of the molecular system. Here, we also considered another pathway for the H extraction, via electrophilic aromatic substitution (S_EAr). Since it is known that electron-rich arenes stabilize a positive charge in the arene rings, the reaction through this pathway should be more facile. However, we found that for neither NO_2 nor OMe para-substituted arenes was the S_EAr pathway favored. The H extraction required 17.6 and 20.0 kcal/mol more, respectively, in comparison with the proposed pathway from Figure 1.

On the other hand, clear differences are observed for the second group of reagents from the substrate screening. Due to the different electronic character of the Ph substituent on the alkyne, in comparison with ODipp, a more difficult scenario was expected in order to achieve the formation of intermediate **II**. However, we observed that the energy barrier defined by the transition state **I-II** is more than 10 kcal/mol lower than that for the rate-determining step of the reaction. From the two fundamental steps of the reaction, we observe that both are highly sensitive to the electronic character of the R_2 group (see Scheme 3). The steps of stereoisomerization and C−C bond

DOI: 10.1021/acs.organomet.8b00102
Organometallics XXXX, XXX, XXX−XXX

Table 1. Energy Data (in kcal/mol) for the Reaction Pathways for the Substrate Screening of Benzosilole Formation[a]

	a	b	c	d	e	f	g	h	i	j	k	l
1+R	0.0	0.0	0.0	0.0	0.0	0.0	0.0	0.0	0.0	0.0	0.0	0.0
I	−8.2	−14.6	−16.7	−15.6	−15.4	−13.7	−7.1	−10.7	−8.7	−12.3	−12.0	−12.0
I-II	3.3	−1.4	−4.1	−2.7	−3.5	−1.5	7.3	−0.7	1.0	−4.9	−7.0	−2.8
II	−11.5	−17.2	−25.9	−18.4	−18.8	−27.7	−9.8	−21.6	−23.9	−23.6	−22.8	−18.9
II-III	12.6	7.0	6.2	5.8	4.9	5.2	28.0	8.8	14.5	5.2	6.4	6.0
III	−23.0	−29.9	−29.9	−30.8	−29.4	−31.6	−13.3	−23.5	−24.1	−30.3	−26.7	−28.3
IV-1	4.4	−2.3	−2.7	−4.5	−5.0	−2.7	16.0	6.0	5.5	−2.2	−1.8	−1.1
1+P	−34.2	−35.0	−35.8	−36.5	−35.4	−38.7	−17.2	−31.6	−32.5	−35.0	−35.1	−33.6

[a]PMe_3 used as the phosphine in all series of data.

formation giving **P** require overcoming energy barriers of 37.8 and 29.3 kcal/mol, respectively, for R_2 = Ph. More than 5 kcal/mol differentiates the stereoisomerization processes with and without the ODipp group. To clearly separate the steric and electronic effects of the substituents, we studied the R_2 = ODipp molecular system. In this case, the only difference in the energy barriers comes from the steric effect of the Si substituents. In the stereoisomerization step, the energy barrier increased from 24.1 to 32.9 kcal/mol due only to sterics. This significant quantitative difference confirms that the energy barrier for R_1 = NPh_2, 32.1 kcal/mol, is guided more by sterics than by the electronic character of the substituent. Thus, the energy barriers are sensitive not only to the electronic character of the alkyne substituent but also to the steric repulsion provided by the Si atom substituents. Moreover, we observed a change in the rds of the reaction, becoming the stereoisomerization step instead of the barrier defined by the transition state **IV-P**.

Experimentally, the reaction with R_2 = O-3,5-Xyl led to a rather poor yield of the product **P**. Computationally the kinetic cost was found to be relatively high, 38.4 kcal/mol, but it is still affordable. Then, to reach good agreement between experiments and computation, we studied the formation of its undesired product (HOXyl) and the reaction for R_2 = ODipp (HODipp), depicted in Figure 4. For R_2 = OXyl, the formation of **P′** goes through an energy barrier of 34.5 kcal/mol starting from **I**, due to intermediate **I″** being less stable than **I**. In comparison with the formation of **P**, where the rds requires 38.4 kcal/mol, the formation of HOXyl is kinetically more favorable. In the R_2 = ODipp case we face the opposite situation. The formation of **P′**, starting from intermediate **I″**, requires 36.0 kcal/mol; meanwhile, the formation of **P** requires 32.9 kcal/mol. Thus, achieving **P** is kinetically more favorable. Moreover, even though **I″** is more stable than **I**, by 0.2 kcal/mol, the energy difference between both species is small enough to not affect the thermodynamic equilibrium, which favors the formation of **P**. These results are in good agreement with experiments.[13]

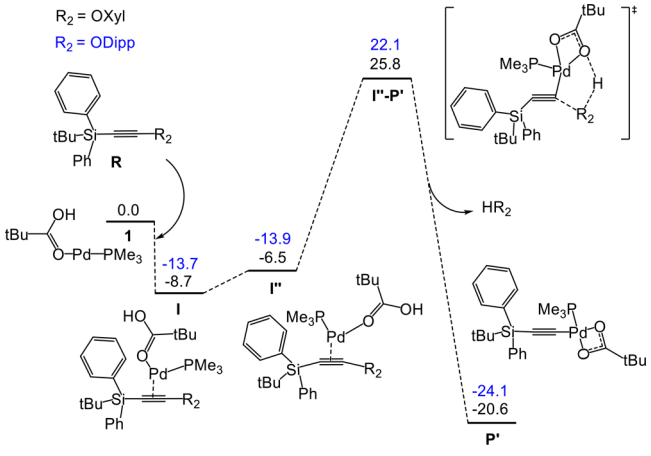

Figure 4. Reaction pathway for the undesired parallel reaction (M06/cc-pVTZ~sdd//BP86-d3/SVP~sdd; Gibbs free energies in kcal/mol referenced to complex **1**).

Since computationally SIMes turned out to be competitive with respect to the most favorable phosphines, experiments were undertaken using substrate **m** (see Table 2). Unexpectedly, the yield decreased to only 4% of the product **P-m** (run 2). When SIMes·HCl was used with KOtBu as a base, the yield was improved by only 1% but the conversion of the substrate became lower (22% vs 11%). To understand this poor performance of the NHC ligand, the undesired reaction studied in Figure 4 was tested for this ligand and was also disfavored, with an energy requirement of 35.0 kcal/mol from **I** to overcome the transition state **I″-P′**, thus being very similar to the phosphine-based systems included in Figure 4.

Table 2. Examination of Benzosilole Formation Using PEt_3 and SIMes Ligands[a]

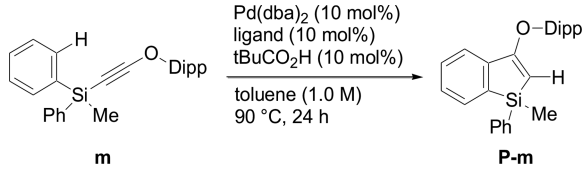

run	ligand	conversion of **m** (%)	yield of **P-m** (%)[b]
1	PEt_3	>99	58
2	SIMes	22	4
3	SIMes·HCl[c]	11	5

[a]Conditions: alkyne **m**, $Pd(dba)_2$ (10 mol %), ligand (10 mol %), $tBuCO_2H$ (10 mol %), in toluene (1.0 M), at 120 °C. [b]Determined by NMR. [c]KO*t*Bu (10 mol %) as an additive.

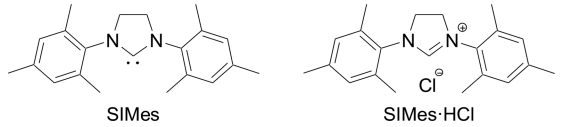

Studies on the sterics and electronics were carried out for the phosphine ligands. First, they confirmed that the computational work on PMe_3 instead of PEt_3 is valid. Further, this study was expanded to compare the phosphines used here by the NHC ligand SIMes. For the sterics, we used the SambVca package developed by Cavallo et al.,[22,23] which allows the direct comparison of phosphines and NHC ligands[24] and, by extension, any ligand.[25] Taking into account the first

DOI: 10.1021/acs.organomet.8b00102
Organometallics XXXX, XXX, XXX−XXX

coordination sphere around the metal is where catalysis occurs, and the buried volume is the amount of the first coordination sphere of the metal occupied by a given ligand, we calculated the total $\%V_{Bur}$ and also a more detailed analysis by evaluating the $\%V_{Bur}$ in the single quadrants around the Pd center and plotted them as steric contour steric maps (Figure S1), see the Supporting Information for further details. Splitting the total $\%V_{Bur}$ into quadrant contributions quantifies any asymmetry in the way the ligand wraps around the metal. Here, this analysis shows how the shape of the reactive pocket is modified on moving from $PtBu_3$ (36.3%) to PPh_3 (29.4%), PEt_3 (27.1%), and PMe_3 (24.1%). Even though the NHC ligand SIMes (37.9%) displays a $\%V_{Bur}$ value close to and even higher than that of the $PtBu_3$ ligand, one quadrant is 2.6% less crowded but is still much more crowded than the active PEt_3-based catalysis. This leads us to conclude, that apart from the effect of the NHC and phosphine on the rds, it is very important to form the active catalytic species **1** from $Pd(dba)_2$ in combination with PivOH, and for this step, the probability is much higher for relatively small phosphines such as PEt_3.

CONCLUSIONS

We have determined the whole reaction mechanism for palladium-catalyzed benzosilole formation using different phenylsilylalkynes as starting materials. We clarified the role of the phosphine, since it became the driving force. Further, this formation is not only a question of sterics; the choice of the electronic nature of this ligand is also crucial to reduce the energy cost of the stereoisomerization step. Even though the rate-determining step is not that affected by the choice of this ligand, its presence becomes mandatory to facilitate the annulation, and a more sterically hindered phosphine slightly facilitates this step. From the substrate scope, we observed not only that the stereoisomerization step becomes the rate-determining step of the reaction but also that the electronic characters of the substituents of the alkyne reagent are much more important than the effects of steric repulsion from nearby groups.

EXPERIMENTAL DETAILS

General Procedure. Substrate **m** (0.10 mmol) was added to a solution of $Pd(dba)_2$ (0.010 mmol), PEt_3 (0.010 mmol), and tBuCO$_2$H (0.010 mmol) in toluene (0.1 mL) prepared in a 3 mL vial under an argon atmosphere in a drybox. The vial was closed with a screw cap, taken outside the drybox, and heated at 90 °C for 24 h. The reaction mixture was filtered through Celite, and the filtrate was evaporated and dried in vacuo. The crude product was analyzed by ^{1}H NMR to determine the yield of the product **P-m** by comparing the reported ^{1}H NMR data of **P-m**.

COMPUTATIONAL DETAILS

All of the DFT static calculations were performed with the Gausian09 set of programs,[26] using the BP86 functional of Becke and Perdew,[27−29] together with the Grimme D3 correction term to the electronic energy.[30] The electronic configuration of the molecular systems was described with the double-ζ basis set with the polarization of Ahlrichs for main-group atoms (SVP keyword in Gaussian),[31] whereas for palladium the small-core quasi-relativistic Stuttgart/Dresden effective core potential, with an associated valence basis set (standard SDD keywords in Gaussian09), was employed.[32−34] The geometry optimizations were performed without symmetry constraints, and analytical frequency calculations enabled the characterization of the located stationary points. These frequencies were used to calculate unscaled zero-point energies (ZPEs) as well as thermal corrections and entropy effects at 298 K. Energies were obtained by single-point calculations on the optimized geometries with the M06 functional and the cc-pVTZ basis set, and solvent effects were estimated with the polarizable continuous solvation model PCM using toluene as solvent.[35] The reported free energies in this work include energies obtained at the M06/cc-pVTZ∼sdd level of theory corrected with zero-point energies, thermal corrections, and entropy effects evaluated at 298 K, achieved at the BP86-D3/SVP∼sdd level.

ASSOCIATED CONTENT

Supporting Information

The Supporting Information is available free of charge on the ACS Publications website at DOI: 10.1021/acs.organomet.8b00102.

Computational details (PDF)

Cartesian coordinates and energies of all species (XYZ)

AUTHOR INFORMATION

Corresponding Authors

*E-mail for Y.M.: yminami@kc.chuo-u.ac.jp.

*E-mail for A.P.: albert.poater@udg.edu.

ORCID

Yasunori Minami: 0000-0002-2435-1951

Tamejiro Hiyama: 0000-0003-4749-1161

Albert Poater: 0000-0002-8997-2599

Notes

The authors declare no competing financial interest.

ACKNOWLEDGMENTS

A.P. thanks the Spanish MINECO for the project CTQ2014-59832-JIN and the EU for a FEDER fund (UNGI08-4 × 10−003). Y.M. and T.H. thank the JST for ACT-C (JPMJCR12Z1). Y.M. also acknowledges a Grant-in-Aid for Challenging Research (Exploratory) (17K19127) from the JSPS.

REFERENCES

(1) Yamaguchi, S.; Tamao, K. *J. Chem. Soc., Dalton Trans.* **1998**, 3693−3702.

(2) Yamaguchi, S.; Tamao, K. *Chem. Lett.* **2005**, *34*, 2−7.

(3) Kobayashi, J.; Kawashima, T. Science of Synthesis Knowledge Updates, 2014/1.

(4) Oestreich, M., Ed.; *Metal-Catalyzed Cross-Coupling Reactions and More*; Thieme: Stuttgart, 2014; pp 351−369.

(5) (a) Matsuda, T.; Kadowaki, S.; Goya, T.; Murakami, M. *Org. Lett.* **2007**, *9*, 133−136. (b) Yabusaki, Y.; Ohshima, N.; Kondo, H.; Kusamoto, T.; Yamanoi, Y.; Nishihara, H. *Chem. - Eur. J.* **2010**, *16*, 5581−5585. (c) Ureshino, T.; Yoshida, T.; Kuninobu, Y.; Takai, K. *J. Am. Chem. Soc.* **2010**, *132*, 14324−14326. (d) Liang, Y.; Zhang, S.; Xi, Z. *J. Am. Chem. Soc.* **2011**, *133*, 9204−9207.

(6) (a) Kuninobu, Y.; Yamauchi, K.; Tamura, N.; Seiki, T.; Takai, K. *Angew. Chem., Int. Ed.* **2013**, *52*, 1520−1522. (b) Shintani, R.; Takagi, C.; Ito, T.; Naito, M.; Nozaki, K. *Angew. Chem., Int. Ed.* **2015**, *54*, 1616−1620. (c) Zhang, Q.-W.; An, K.; Liu, L.-C.; Yue, Y.; He, W. *Angew. Chem., Int. Ed.* **2015**, *54*, 6918−6921. (d) Murai, M.; Matsumoto, K.; Takeuchi, Y.; Takai, K. *Org. Lett.* **2015**, *17*, 3102−3105. (e) Murai, M.; Okada, R.; Nishiyama, A.; Takai, K. *Org. Lett.* **2016**, *18*, 4380−4383. (f) Zhang, Q.-W.; An, K.; Liu, L.-C.; Guo, S.; Jiang, C.; Guo, H.; He, W. *Angew. Chem., Int. Ed.* **2016**, *55*, 6319−6323.

(7) (a) Wu, B.; Yoshikai, N. *Org. Biomol. Chem.* **2016**, *14*, 5402−5416. (b) Mochida, K.; Shimizu, M.; Hiyama, T. *J. Am. Chem. Soc.* **2009**, *131*, 8350−8351. (c) Zhang, Q.-W.; An, K.; He, W. *Angew. Chem., Int. Ed.* **2014**, *53*, 5667−5671. (d) Omann, L.; Oestreich, M. *Organometallics* **2017**, *36*, 767−776.

(8) (a) Arii, H.; Nakabayashi, K.; Mochida, K.; Kawashima, T. *Molecules* **2016**, *21*, 999. (b) Matsuda, T.; Kadowaki, S.; Murakami, M.

DOI: 10.1021/acs.organomet.8b00102
Organometallics XXXX, XXX, XXX−XXX

Chem. Commun. **2007**, *43*, 2627−2629. (c) Matsuda, T.; Kadowaki, S.; Yamaguchi, Y.; Murakami, M. *Chem. Commun.* **2008**, *44*, 2744−2746. (d) Ilies, L.; Tsuji, H.; Sato, Y.; Nakamura, E. *J. Am. Chem. Soc.* **2008**, *130*, 4240−4241. (e) Matsuda, T.; Yamaguchi, T.; Shigeno, M.; Sato, S.; Murakami, M. *Chem. Commun.* **2011**, *47*, 8697−8699. (f) Matsuda, T.; Ichioka, Y. *Org. Biomol. Chem.* **2012**, *10*, 3175−3177. (g) Ilies, L.; Tsuji, H.; Nakamura, E. *Org. Lett.* **2009**, *11*, 3966−3968. (h) Ilies, L.; Sato, Y.; Mitsui, C.; Tsuji, H.; Nakamura, E. *Chem. - Asian J.* **2008**, *41*, 1376−1381.

(9) Ouyang, K.; Liang, Y.; Xi, Z. *Org. Lett.* **2012**, *14*, 4572−4575.

(10) Matsuda, T.; Yamaguchi, Y.; Murakami, M. *Synlett* **2008**, *2008*, 561−564.

(11) Teo, W. J.; Wang, C.; Tan, Y. W.; Ge, S. *Angew. Chem., Int. Ed.* **2017**, *56*, 4328−4332.

(12) (a) Liang, Y.; Geng, W.; Wei, J.; Xi, Z. *Angew. Chem., Int. Ed.* **2012**, *51*, 1934−1937. (b) Tobisu, M.; Onoe, M.; Kita, Y.; Chatani, N. *J. Am. Chem. Soc.* **2009**, *131*, 7506−7507. (c) Shirakawa, E.; Masui, S.; Narui, R.; Watabe, R.; Ikeda, D.; Hayashi, T. *Chem. Commun.* **2011**, *47*, 9714−9716.

(13) Minami, Y.; Noguchi, Y.; Hiyama, T. *J. Am. Chem. Soc.* **2017**, *139*, 14013−14016.

(14) Itami, K.; Terakawa, K.; Yoshida, J.; Kajimoto, O. *Bull. Chem. Soc. Jpn.* **2004**, *77*, 2071−2080.

(15) Itami, K.; Terakawa, K.; Yoshida, cJ.-i.; Kajimoto, O. *J. Am. Chem. Soc.* **2003**, *125*, 6058−6059.

(16) Yu, Z.; Lan, Y. *J. Org. Chem.* **2013**, *78*, 11501−11507.

(17) (a) Rünzi, T.; Tristschler, U.; Roesle, P.; Gottker-Schnetmann, I.; Moller, H. M.; Caporaso, L.; Poater, A.; Cavallo, L.; Mecking, S. *Organometallics* **2012**, *31*, 8388−8406. (b) Meconi, G. M.; Vummaleti, S. V. C.; Luque-Urrutia, J. A.; Belanzoni, P.; Nolan, S. P.; Jacobsen, H.; Cavallo, L.; Solà, M.; Poater, A. *Organometallics* **2017**, *36*, 2088−2095.

(18) Shen, R.; Chen, T.; Zhao, Y.; Qiu, R.; Zhou, Y.; Yin, S.; Wang, X.; Goto, M.; Han, L.-B. *J. Am. Chem. Soc.* **2011**, *133*, 17037−17044.

(19) (a) Brady, K. A.; Nile, T. A. *J. Organomet. Chem.* **1981**, *206*, 299−304. (b) Ojima, I.; Clos, N.; Donovan, R. J.; Ingallina, P. *Organometallics* **1990**, *9*, 3127−3133.

(20) Murakami, M.; Yoshida, T.; Kawanami, S.; Ito, Y. *J. Am. Chem. Soc.* **1995**, *117*, 6408−6409.

(21) (a) Czerwinski, P.; Molga, E.; Cavallo, L.; Poater, A.; Michalak, M. *Chem. - Eur. J.* **2016**, *22*, 8089−8094. (b) Leitgeb, A.; Abbas, M.; Fischer, R. C.; Poater, A.; Cavallo, L.; Slugovc, C. *Catal. Sci. Technol.* **2012**, *2*, 1640−1643.

(22) Poater, A.; Cosenza, B.; Correa, A.; Giudice, S.; Ragone, F.; Scarano, V.; Cavallo, L. *Eur. J. Inorg. Chem.* **2009**, *2009*, 1759−1766.

(23) Falivene, L.; Credendino, R.; Poater, A.; Petta, A.; Serra, L.; Oliva, R.; Scarano, V.; Cavallo, L. *Organometallics* **2016**, *35*, 2286−2293.

(24) (a) Jacobsen, H.; Correa, C.; Poater, A.; Costabile, C.; Cavallo, L. *Coord. Chem. Rev.* **2009**, *253*, 687−703. (b) Poater, A.; Falivene, L.; Urbina-Blanco, C. A.; Manzini, S.; Nolan, S. P.; Cavallo, L. *Dalton Trans.* **2013**, *42*, 7433−7439. (c) Ahmed, S. M.; Poater, A.; Childers, M. I.; Widger, P. C. B.; LaPointe, A. M.; Lobkovsky, E. B.; Coates, G. W.; Cavallo, L. *J. Am. Chem. Soc.* **2013**, *135*, 18901−18911.

(25) (a) Richmond, C. J.; Matheu, R.; Poater, A.; Falivene, L.; Benet-Buchholz, J.; Sala, X.; Cavallo, L.; Llobet, A. *Chem. - Eur. J.* **2014**, *20*, 17282−17286. (b) Rouen, M.; Queval, P.; Borré, E.; Falivene, L.; Poater, A.; Berthod, M.; Hugues, F.; Cavallo, L.; Baslé, O.; Olivier-Bourbigou, H.; Mauduit, M. *ACS Catal.* **2016**, *6*, 7970−7976. (c) Luque-Urrutia, J. A.; Poater, A. *Inorg. Chem.* **2017**, *56*, 14383−14387.

(26) Frisch, M. J.; Trucks, G. W.; Schlegel, H. B.; Scuseria, G. E.; Robb, M. A.; Cheeseman, J. R.; Scalmani, G.; Barone, V.; Mennucci, B.; Petersson, G. A.; Nakatsuji, H.; Caricato, M.; Li, X.; Hratchian, H. P.; Izmaylov, A. F.; Bloino, J.; Zheng, G.; Sonnenberg, J. L.; Hada, M.; Ehara, M.; Toyota, K.; Fukuda, R.; Hasegawa, J.; Ishida, M.; Nakajima, T.; Honda, Y.; Kitao, O.; Nakai, H.; Vreven, T.; Montgomery, J. A., Jr.; Peralta, J. E.; Ogliaro, F.; Bearpark, M.; Heyd, J. J.; Brothers, E.; Kudin, K. N.; Staroverov, V. N.; Kobayashi, R.; Normand, J.; Raghavachari, K.; Rendell, A.; Burant, J. C.; Iyengar, S. S.; Tomasi, J.; Cossi, M.; Rega, N.; Millam, N. J.; Klene, M.; Knox, J. E.; Cross, J. B.; Bakken, V.; Adamo, C.; Jaramillo, J.; Gomperts, R.; Stratmann, R. E.; Yazyev, O.; Austin, A. J.; Cammi, R.; Pomelli, C.; Ochterski, J. W.; Martin, R. L.; Morokuma, K.; Zakrzewski, V. G.; Voth, G. A.; Salvador, P.; Dannenberg, J. J.; Dapprich, S.; Daniels, A. D.; Farkas, Ö.; Foresman, J. B.; Ortiz, J. V.; Cioslowski, J.; Fox, D. J. *Gaussian 09, Revision E.01*; Gaussian, Inc., Wallingford, CT, 2009.

(27) Becke, A. *Phys. Rev. A: At., Mol., Opt. Phys.* **1988**, *38*, 3098−3100.

(28) Perdew, J. P. *Phys. Rev. B: Condens. Matter Mater. Phys.* **1986**, *33*, 8822−8824.

(29) Perdew, J. P. *Phys. Rev. B: Condens. Matter Mater. Phys.* **1986**, *34*, 7406−7406.

(30) Grimme, S.; Antony, J.; Ehrlich, S.; Krieg, H. *J. Chem. Phys.* **2010**, *132*, 154104.

(31) Schäfer, S.; Horn, H.; Ahlrichs, R. *J. Chem. Phys.* **1992**, *97*, 2571−2577.

(32) Haussermann, U.; Dolg, M.; Stoll, H.; Preuss, H.; Schwerdtfeger, P.; Pitzer, R. M. *Mol. Phys.* **1993**, *78*, 1211−1224.

(33) Küchle, W.; Dolg, M.; Stoll, H.; Preuss, H. *J. Chem. Phys.* **1994**, *100*, 7535−7542.

(34) Leininger, T.; Nicklass, A.; Stoll, H.; Dolg, M.; Schwerdtfeger, P. *J. Chem. Phys.* **1996**, *105*, 1052−1059.

(35) (a) Barone, V.; Cossi, M. *J. Phys. Chem. A* **1998**, *102*, 1995−2001. (b) Tomasi, J.; Persico, M. *Chem. Rev.* **1994**, *94*, 2027−2094.

DOI: 10.1021/acs.organomet.8b00102
Organometallics XXXX, XXX, XXX−XXX